Satellite observations of desert dust-induced Himalayan snow darkening

Ritesh Gautam,[1,2] N. Christina Hsu,[2] William K.-M. Lau,[2] and Teppei J. Yasunari[1,2]

Received 25 November 2012; revised 28 January 2013; accepted 5 February 2013; published 11 March 2013.

[1] The optically thick aerosol layer along the southern edge of the Himalaya has been subject of several recent investigations relating to its radiative impacts on the South Asian summer monsoon and regional climate forcing. Prior to the onset of summer monsoon, mineral dust from southwest Asian deserts is transported over the Himalayan foothills on an annual basis. Episodic dust plumes are also advected over the Himalaya, visible as dust-laden snow surface in satellite imagery, particularly in western Himalaya. We examined spectral surface reflectance retrieved from spaceborne MODIS observations that show characteristic reduction in the visible wavelengths (0.47 μm) over western Himalaya, associated with dust-induced solar absorption. Case studies as well as seasonal variations of reflectance indicate a significant gradient across the visible (0.47 μm) to near-infrared (0.86 μm) spectrum (VIS-NIR), during premonsoon period. Enhanced absorption at shorter visible wavelengths and the resulting VIS-NIR gradient is consistent with model calculations of snow reflectance with dust impurity. While the role of black carbon in snow cannot be ruled out, our satellite-based analysis suggests the observed spectral reflectance gradient dominated by dust-induced solar absorption during premonsoon season. From an observational viewpoint, this study underscores the importance of mineral dust deposition toward darkening of the western Himalayan snow cover, with potential implications to accelerated seasonal snowmelt and regional snow albedo feedbacks. **Citation:** Gautam R., N. C. Hsu, W. K.-M. Lau, and T. J. Yasunari (2013), Satellite observations of desert dust-induced Himalayan snow darkening, *Geophys. Res. Lett.*, *40*, 988–993, doi:10.1002/grl.50226.

1. Introduction

[2] Mineral dust deposition over snow can lead to accelerated snowmelt [*Painter et al*., 2010] due to snow darkening [*Warren and Wiscombe*, 1980], i.e., reduction of snow albedo due to enhanced solar absorption. Climate modeling simulations indicate absorbing aerosols, such as dust and black carbon (BC), as major snow darkening agents leading to enhanced climate warming and accelerated snowmelt in the Northern Hemisphere, especially in Eurasia including the Himalaya-Tibetan Plateau (HTP) [*Flanner et al*., 2009]. In addition to triggering snow albedo feedback processes, absorbing aerosols are also suggested to cause accelerated glacier retreat in the HTP, coinciding with increased BC emissions in south and east Asia in recent decades [*Xu et al*., 2009].

[3] The HTP are among the largest ice-covered regions of the Earth's surface, outside the poles, and their glaciers form source of major rivers in Asia, which serve a large population base downstream. Recent studies have shown tropospheric warming [*Ramanathan et al*., 2007; *Gautam et al*., 2009], accelerated snowmelt over the HTP, as well as perturbations to the Asian summer monsoon rainfall—partly due to enhanced solar absorption by natural and anthropogenic aerosols [*Lau et al*., 2006, 2010]. Both the absorbing aerosol deposition and aerosol-induced atmospheric warming [*Flanner et al*., 2009; *Lau et al*., 2010; *Qian et al*., 2011; *Yasunari et al*., 2012] over snow are suggested to be important factors toward accelerated snowmelt in the HTP, particularly during the premonsoon season (May–June). Prior to the onset of the summer monsoon, westerly wind-blown mineral dust from southwest Asian deserts and as far as from the Arabian Peninsula is transported over south Asia in multiple dust events each year. As a result, the aerosol loading peaks over northern India, during the transition of spring to summer months, with episodic dust influence observed to extend over the Himalaya, particularly in western Himalaya (WH) [*Hegde et al*., 2007; *Prasad and Singh*, 2007; *Gautam et al*., 2011]. Mixed with anthropogenic pollution, mineral dust forms a widespread vertically extended haze against the southern slopes of the Himalaya. Episodic dust plumes are also advected over the Himalaya, leading to dust-laden snow surface, as observed in satellite imagery (Figure 1).

[4] In the HTP, ice core record have indicated peak annual dust concentrations prior to the summer monsoon season, with enhanced dust deposition during periods of dry/drought conditions over southern Asia [*Thompson et al*., 2000]. A recent study demonstrated the capability of satellite-derived estimation of dust radiative forcing in snow and showed large forcings over the Himalaya, from Moderate Resolution Imaging Spectroradiometer (MODIS) [*Painter et al*., 2012]. The southern edge of the HTP, especially western Himalaya, is close to dust source regions; yet the possible effects of mineral dust deposition on snow albedo in the Himalaya is not well understood due to lack of observations. In this paper, we focus on the role of mineral dust toward snow darkening in the Himalaya. From an observational viewpoint, this study utilizes spaceborne measurements of reflectance over the Himalayan snow cover to infer the reduction of snow albedo by dust-induced solar absorption.

All Supporting Information may be found in the online version of this article.

[1]GESTAR/Universities Space Research Association, Columbia, Maryland, USA.
[2]NASA Goddard Space Flight Center, Greenbelt, Maryland, USA.

Corresponding author: Ritesh Gautam, NASA Goddard Space Flight Center, Greenbelt, MD 20771, USA. (Ritesh.Gautam@nasa.gov)

0094-8276/13/10.1002/grl.50226

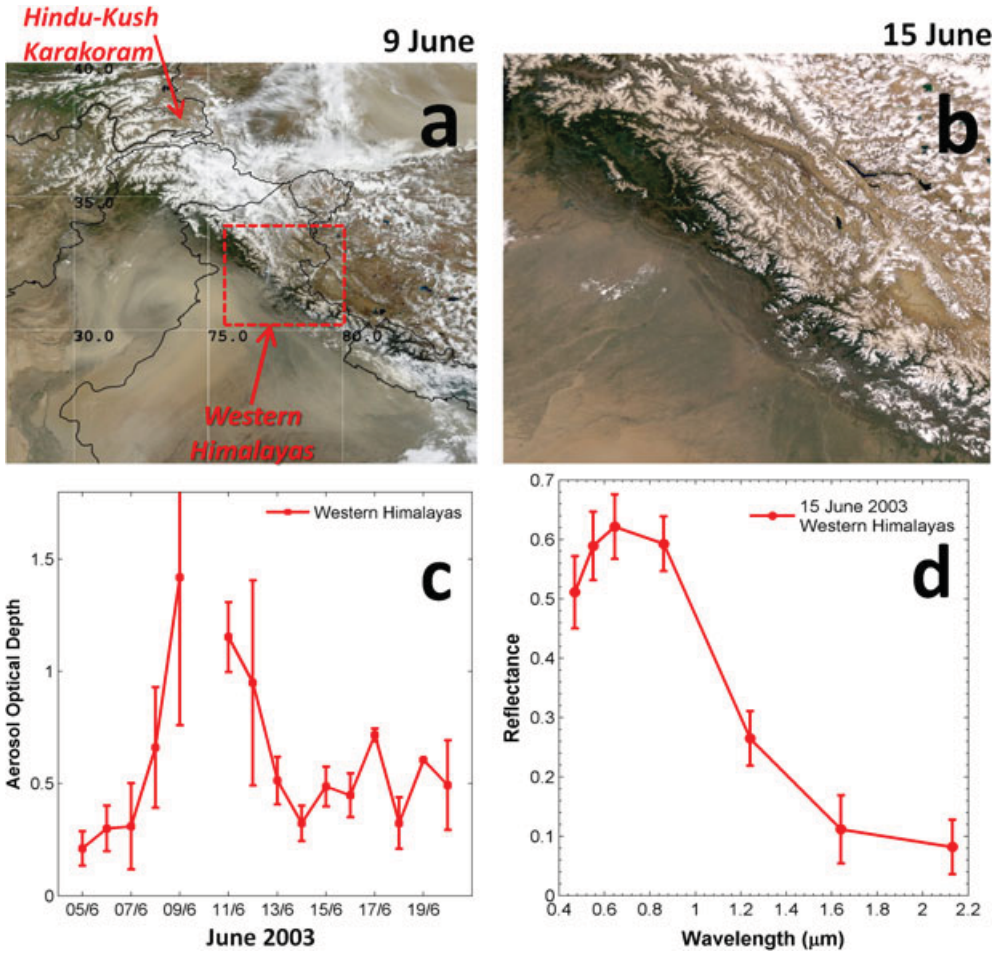

Figure 1. (a) Satellite image of a major dust outbreak over south Asia, on 9 June 2003 from Terra/MODIS, indicating visibly dust-laden snow surface in the western Himalaya (WH); (b) zoom-in over WH on 15 June 2003; (c) daily AOD variations over the foothills, south of the WH snow cover; (d) MODIS spectral surface reflectance on 15 June indicating the VIS-NIR gradient for WH (30°N–34°N, 76°E–80°E), with error bars of $\pm 1\sigma$ representing pixel-level variability.

2. Satellite Data Set

[5] We use Terra/MODIS spectral surface reflectance data (MOD09) over the Himalayan snow-covered region. The MODIS surface reflectance (R) is retrieved after performing corrections for atmospheric effects (gaseous absorption, molecular and aerosol scattering) [*Vermote et al.*, 2002]. Reflectances from MODIS land bands in swath format, at seven wavelengths from 0.47 to 2.1 μm, were mapped onto a 0.01° × 0.01° spatial resolution (~1.2 × 1.2 km pixel size). In order to focus over snow surface, MODIS snow cover fraction (SCF) product was used as an indicator of fractional snow cover available within a MODIS footprint, at a spatial resolution of 500 m. Daily SCF swath data were also gridded to ~1.2 km pixel size for consistent colocation with reflectance data. The MODIS SCF is derived from the normalized difference snow index [*Salomonson and Appel*, 2004] with overall accuracy of snow cover swath products reported as above 90% [*Hall and Riggs*, 2007]. A recent study, however, suggests that the MODIS SCF has lower accuracy than previously reported with an RMSE of 0.23 [*Rittger et al.*, 2012]. The SCF data set was further filtered and only considered for pixels with >99% snow fraction, in order to constrain our analysis for highly snow covered regions. An additional threshold of 0.3 was introduced, for $R_{0.47\mu m}$ (below which all spectral reflectance values are not considered in the analysis), to minimize subpixel contamination of snow (with, e.g., vegetation/bare soil) in inferring the role of dust absorption toward reduction of reflectance.

3. Results

3.1. Satellite Observations of Snow Darkening

[6] Prior to the onset of the Indian summer monsoon, the Indo-Gangetic Plains (IGP), along the southern edge of the Himalaya, are strongly influenced by westerly wind-driven dust storms on an annual basis (April–June). Figure 1a shows a satellite image of a major dust outbreak over south Asia, on 9 June 2003, from Terra/MODIS. The circulating dust plume appears to have originated over the Thar Desert in northwestern India and is transported over the IGP. The dust plume is also seen to be advected over the elevated western Himalaya (WH) leading to visibly dust-laden snow surface (Figure 1a). A zoom-in over WH further reveals the extent of the plume toward observed darkening over the snow cover, with significant dust loading also apparent in the mountain valleys as well as further south over the plains (Supplementary Figure 1).

[7] The anomalous high aerosol loading, associated with the dust plume, is shown in Figure 1c from daily variations of Terra/MODIS Aerosol Optical Depth (AOD) over a 1° × 1° region (31°N–32°N, 77°E–78°E) south of the snow cover (aerosol retrievals over snow are not available from MODIS). The aerosol loading is generally low (AOD ~ 0.2–0.3) prior to the dust outbreak (5–7 June) and sharply increases thereafter during the dust outbreak resulting in fourfold increase causing highest AOD on 9 June. The uncertainty of MODIS AOD over land is reported to be within $\pm 0.05 \pm 0.15$*AOD [*Levy et al*., 2010]. After the passage of dust storm, the AOD significantly reduced to lower values during 13–20 June. The persistence of darkening is further observed on 15 June, i.e., few days after the dust event (Figure 1b). The background conditions appear to be relatively clean on 15 June over the IGP and the mountain valley (as indicated by lower AOD, see Supplementary Figure 1), compared to 9 June; however, the WH snow cover still appears to be darkened due to probable dust deposition.

[8] The corresponding spectral surface reflectance (0.47–2.1 μm) over the WH snow cover for 15 June is shown in Figure 1d. A significant gradient of ~9% absolute difference in the visible–near infrared (0.47–0.86 μm, hereafter VIS-NIR) spectrum is found, with enhanced solar absorption at shorter visible wavelength. Since dust aerosols can be significantly absorbing at shorter visible wavelengths, it is reasonable to expect that dust deposition on snow could lead to the observed gradient. In relation to contaminated snow with dust impurity, some of the earliest works [*Warren and Wiscombe*, 1980] have shown that dust particles effectively reduce snow albedo, especially around 0.4 μm, thus causing a significant gradient in the VIS-NIR spectrum. The shorter visible wavelengths are most sensitive to light-absorbing impurity, and therefore, the possibility of dust-induced absorption and related feedback processes toward accelerated snowmelt cannot be ruled out, especially with the VIS-NIR gradient over WH, as shown here.

[9] It is worth noting that the observed reflectance is in the range 0.5–0.6 in VIS-NIR, which is substantially lower than that of pure/clean snow (typically above 0.95 in VIS-NIR). The reflectance is lower, during our study period, because it is observed well into the snowmelt season over the Himalaya. Snowmelt is generally characterized by wet snow and is associated with larger snow grain size (snow aging); combined with the accumulation of impurities, the net effect is an overall reduction of snow albedo [*Wiscombe and Warren*, 1980]. Additionally, snowmelt along with exposure of glacier ice is also characterized by reduced albedo (0.5–0.6 in VIS-NIR) as indicated by field-based spectral measurements [*Hall et al*., 1988]. However, snow at higher elevations would remain dry and new snowfall can occur; therefore, the observed lower reflectance is a likely indicator that aged/contaminated snow dominates the satellite observed region of WH (30°N–34°N, 76°E–80°E). In addition, the MOD09 surface reflectance product, used here, is an apparent surface reflectance product, assuming a level surface—therefore, the dynamic range of the signal is affected by topography.

[10] In general, a gradual accumulation of dustiness over WH was noted in satellite imagery from April to June, with the influence of dust largest during May–June. This likely deposition period of dust over snow is consistent with the seasonal variation of accumulation of aerosols over the IGP and the Himalayan foothills, when dust loading dominates the column AOD. Dust activity begins around April over northern India (associated with enhanced convection) and peaks during May–June, i.e., prior to the onset of the summer monsoon. Before the peak dusty period, a contrasting and relatively flat VIS-NIR spectrum is found for 27 May over WH (unlike the strong VIS-NIR gradient for 15 June), with visibly brighter snowpack in WH suggesting relatively lower contamination, in low background aerosol loading conditions (see Supplementary Figure 1). In order to better understand the possible response of accumulation of dust on snow albedo, the seasonal variation of reflectance is studied from winter to summer. Figure 2a shows ~15-day averaged spectral surface reflectance from February to June over the WH snow cover (reflectances are normalized to cosine of solar zenith angle). The reflectance generally reduces from February to June as the transition occurs from winter-spring-summer months and results in a near-systematic decrease in the overall spectral reflectance from 0.47 to 2.1 μm, suggesting the progression of snow aging during the 5-month period. Seasonal variations suggest coarsening of snow grain size, due to snow aging (and progressive snowmelt), which reduces the reflectance in the longer wavelengths (>1.0 μm), and reduction at shorter visible wavelengths due to accumulation of impurities (especially at 0.47 μm). The seasonal variation also shows the emergence of VIS-NIR gradient between 0.47 and 0.86 μm during June over the dust-laden western Himalayan snow cover. This noted spectral gradient is quite contrasting when compared to that with April–May and earlier into the winter-spring period when the spectral shape is relatively flat or even associated with visible reflectances exceeding that at 0.86 μm (NIR) (suggesting presence of clean snow due to winter time new snow accumulation). While a flat VIS-NIR spectrum exhibits some absorption due to snow impurity, a significant VIS-NIR gradient as observed here, with lower reflectance at shorter visible wavelength, is likely associated with dust-dominated contamination in snow [*Warren and Wiscombe*, 1980], thus suggesting increased dust deposition in late premonsoon relative to winter-spring over the western Himalaya. We also found even lower values of reflectance (0.37 ± 0.06) for MODIS band 8 (0.412 μm) during the dusty period (1–15 June) indicating a stronger VIS-NIR gradient. However, $R_{0.412\ \mu m}$ is not available for bright snow pixels in the selected WH region, as this MODIS channel saturates for bright snow/clouds, and therefore, the reported $R_{0.412\ \mu m}$ is biased low.

[11] The VIS-NIR gradient is also evident in the spatial distribution of absolute difference between $R_{0.47}$ and $R_{0.86}$ (Figure 2b), averaged for 6–15 June 2003, with the dust-laden WH snow covered regions characterized largely by negative differences. The variability in the spatial pattern, with the discernible north–south gradient, is likely due to the transport pathway of westerly wind-blown desert dust such that the southwestern Himalaya-Hindu Kush are subjected to greater dust influx leading to higher snow albedo reduction. Additionally, the southwestern edge of the Himalaya may also act as a barrier for the intrusion of dust-laden air mass into the northern regions of Karakoram. These observations are also, in general, consistent with a case study of dust-radiative forcing in snow over the Himalaya, shown by *Painter et al*. 2012, derived using

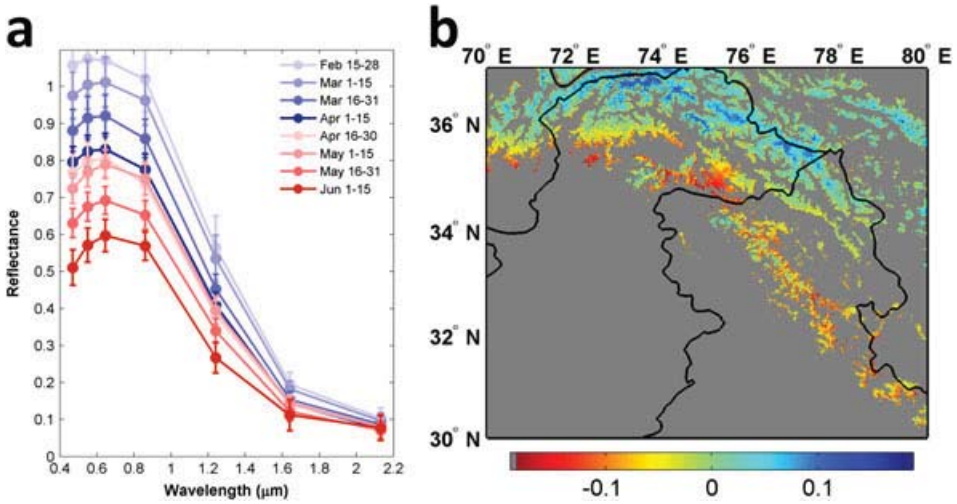

Figure 2. (a) Seasonal variations of spectral surface reflectance (from February to June), shown as 15 day averages over WH snow cover (error bars denote $\pm 1\sigma$ standard deviation). (b) Absolute difference of surface reflectance between 0.47 and 0.86 μm, averaged for 6–15 June 2003. Positive difference is generally found over the Karakoram, while dust-laden WH and southern Hindu-Kush region are characterized by negative differences. Shaded region in gray represents no data/non-snow-covered regions.

MODIS data. Furthermore, the VIS-NIR gradient is also found for top-of-atmosphere (TOA) reflectance (see Supplementary Figure 2), suggesting the response of dust-induced snow darkening observed at TOA. Here the VIS-NIR gradient at TOA may be amplified by atmospheric forcing due to dust overlying snow, leading to enhanced absorption at 0.47 μm (as later discussed in section 4), with its dynamic range different than that induced by dust deposition toward snow darkening.

3.2. Snow Reflectance Modeling

[12] To further illustrate the effect of dust deposition leading to reduced snow reflectance, we modeled the reflectance of snow mixed with varying concentrations of dust impurity. We use the analytical bidirectional reflectance distribution function model of snow reflectance, which is particularly suited to multispectral remote sensing observations [*Kokhanovsky and Breon*, 2012], and accounts for sensitivity to snow grain size and impurity in snow. The snow reflectance model and its various inputs are described in the supplementary material. One of the inputs to the model is imaginary part (m_{im}) of the complex refractive index of ice, which is obtained from *Warren and Brandt* [2008]. This model input (m_{im}) is modified to represent the imaginary part (m_{imd}) of the complex refractive index of ice contaminated with dust by the following procedure. First, the absorption coefficient (k) for dust-contaminated snow was calculated using the formulation described in *Yasunari et al*. [2011], which includes inputs of dust mass absorption coefficients (shown in Supplementary Figure 3) and mass concentration of dust impurity in snow, as shown using different levels of impurity concentration in Figure 3a. The imaginary part (m_{imd}) of the complex refractive of ice, contaminated with dust, is then obtained from the absorption coefficient (k) of dust-contaminated snow using the general approximation by *Wiscombe and Warren* [1980]:

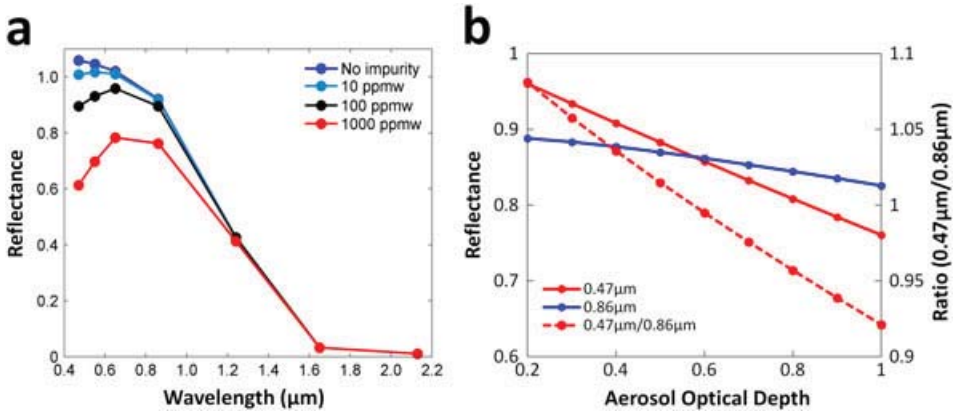

Figure 3. Model sensitivity calculations of reflectance of (a) pure snow mixed with varying levels of dust impurity at solar zenith, viewing zenith, and relative azimuth angles of 30°, 20°, and 140°, respectively, and (b) reduction of TOA reflectance due to dust above clean snow, with VIS-NIR gradient shown as ratio of reflectance between 0.47 and 0.86 μm (secondary y axis).

$$k = 4\pi m_{\mathrm{imd}}/\lambda.$$

[13] Other inputs to the snow reflectance model include information about Sun-satellite geometry (Figure 3a). Sensitivity calculations were performed for the seven MODIS wavelengths, shown in Figures 1 and 2, for a fixed small snow grain radius of 140 μm, representing pure snow. Figure 3a shows the calculated snow reflectance with no impurity (blue) and with varying concentrations of dust impurity in snow: 10 ppmw (cyan), 100 ppmw (black), and 1000 ppmw (red). Clearly, the influence of dust is simulated toward significant reduction of the visible wavelengths, especially at 0.47 μm, resulting in the VIS-NIR gradient. This spectral gradient is similar to that observed over western Himalaya from MODIS data showing enhanced absorption causing the VIS-NIR gradient, with a peak in the red band (0.65 μm) and enhanced absorption at shorter visible wavelength (0.47 μm) (Figures 1 and 2). Objective of this sensitivity study, shown in Figure 3a, is to show the radiative effect of light-absorbing dust toward reduction of snow albedo, in terms of the gradient, thus complementing satellite observations. Additionally, the selection of input dust (or other aerosol) optical model would also perturb the VIS-NIR gradient. Generally, a strongly absorbing dust model implies a stronger gradient and increased snow albedo reduction and vice versa. Therefore, knowledge of regional aerosol optical properties in the high Himalaya is crucial in determining associated radiative impacts on snow albedo. Furthermore, this region is also in vicinity of the IGP where high BC emissions are prevalent, and therefore, it is likely that BC, mixed with dust, may also cause reduction of snow albedo in the Himalaya. Although BC is a strong absorber and effectively reduces snow albedo, its absorption spectrum in VIS-NIR is relatively flat and causes snow albedo reduction more uniformly across wavelengths in VIS-NIR [*Warren and Wiscombe*, 1980], compared to that of mineral dust which is strongly absorbing in the blue bands (0.4–0.47 μm). With respect to the strong spectral gradient observed over WH (Figures 1 and 2), we infer that this is associated with a dust-dominated deposition scenario in the premonsoon season. Black carbon is relevant toward snow darkening and may amplify the overall albedo reduction, but from a remote sensing approach that we show here, dust-induced snow darkening seems to have a more dominant signal with reference to the spectral shape of reflectance.

4. Discussions and Summary

[14] Similar to the radiative effect of dust impurity in snow, dust above clean snow can also lead to enhanced absorption at shorter wavelengths, causing a VIS-NIR gradient at TOA. Figure 3b shows radiative transfer model (RTM)–calculated reduction of TOA reflectance at 0.47 μm, as a function of dust optical depth in the atmosphere, representing radiative effect of dust loading above clean snow. Here the 6S RTM [*Vermote et al*., 1997] was used to calculate the radiative impact of dust overlying snow. The same dust optical model, corresponding to dust impurity in Figure 3a, is used as input to the dust-overlying snow RTM calculations, in order to be consistent between the two scenarios. The aerosol single scattering albedo (SSA) at 0.47 μm is ~0.91, averaged for four dust size bins within 0.1–10 μm, representing moderately absorbing dust (shown in Supplementary Figure 3). In comparison to the shorter wavelength, reflectance at 0.86 μm is not very sensitive to dust loading resulting in the simulated gradient associated with enhanced absorption at 0.47 μm at higher optical depths, as indicated by the ratio $(0.47\,\mu m/0.86\,\mu m) < 1$ (secondary y axis in Figure 3b). This is due to the weakly absorbing property of the dust model (SSA at 0.86 μm is 0.97) used here. The darkening at the shorter wavelength is caused due to multiple reflections, leading to enhanced absorption, between a bright surface (snow in this case) and the overlying absorbing aerosol layer (dust above snow). Here the VIS-NIR gradient at TOA, is largely a function of aerosol optical properties (e.g., SSA) and the underlying snow surface characteristics (pure vs. aged/contaminated snow), and its detection would depend on these two factors. Regarding the efficacy of dust-induced reduction, we think that, in comparison to dust above snow, dust deposition would have larger snow albedo reduction during premonsoon period. This is because once dust is deposited (given there is less new snow accumulation during the premonsoon snowmelt season), it may induce a longer-term reduction of snow albedo by darkening and in turn lead to a positive feedback toward accelerated snowmelt. On the contrary, dust above snow could have measurable instantaneous radiative warming; however, once the dust layer is advected away or deposited, the atmospheric forcing significantly reduces.

[15] Finally, this observational study underscores the role of mineral dust deposition in the reduction of the western Himalayan snow albedo. While satellite data have known limitations associated with complex terrain effects, subpixel contamination, and atmospheric correction, they could be useful in inferring and mapping the large-scale extent of dust deposition on snow in complex/remote environments where in situ measurements are not readily available, as demonstrated in the present study and in *Painter et al*. [2012]. Nonetheless, detailed ground-based measurements of partitioning of snow impurities and atmospheric aerosol composition, particularly dust and BC, as well as coincident snow albedo characterization in the western Himalaya are required to quantify the aerosol-snow radiative coupling in order to further understand effects of snow darkening. In addition to the critical role of deposition in snow darkening, associated with increasing anthropogenic emissions in south and east Asia, our study further suggests that naturally occurring transported dust can also potentially influence seasonal snow albedo feedback processes during the premonsoon period on an interannual scale. With reference to the monsoon, climate modeling has suggested several absorbing aerosol-mediated pathways in perturbing the monsoon circulation [*Ramanathan et al*., 2005; *Lau et al*., 2006; *Meehl et al*., 2008; *Wang et al*., 2009]. Thus, the role of mineral dust deposition, in influencing seasonal warming over the Himalaya, may also contribute toward the overall absorbing aerosol impact on the summer monsoon circulation over southern Asia. Of particular importance and with relevance to dust influx is the western Himalaya—source of two major rivers (Indus and Ganges), which provide major freshwater resource to the downstream population of southern Asia.

[16] **Acknowledgments.** This work is supported by the Terra/Aqua Science Program, NASA Headquarters. MODIS science teams are

acknowledged for provision of satellite data. We thank Mark Flanner and Charles Zender for providing dust optical properties data set, which were used in our snow reflectance model simulations, and Andrew Sayer for his suggestions and useful discussions related to snow reflectance modeling. Thomas Painter and one anonymous reviewer are thanked for helpful comments in improving an earlier version of the manuscript.

References

Flanner, M. G., C. S. Zender, P. G. Hess, N. M. Mahowald, T. H. Painter, V. Ramanathan, and P. J. Rasch (2009), Springtime warming and reduced snow cover from carbonaceous particles, *Atmos. Chem. Phys.*, *9*, 2481–2497, doi:10.5194/acp-9-2481-2009.

Gautam, R., N. C. Hsu, K.-M. Lau, S.-C. Tsay, and M. Kafatos (2009), Enhanced pre-monsoon warming over the Himalayan-Gangetic region from 1979 to 2007, *Geophys. Res. Lett.*, *36*, L07704, doi:10.1029/2009GL037641.

Gautam, R., et al. (2011), Accumulation of aerosols over the Indo-Gangetic plains and southern slopes of the Himalayas: distribution, properties and radiative effects during the 2009 premonsoon season, *Atmos. Chem. Phys.*, *11*, 12841–12863, doi:10.5194/acp-11-12841-2011.

Hall, D. K., and G. A. Riggs (2007), Accuracy assessment of the MODIS snow products, *Hydrol. Processes*, *21*, 1534–1547, doi:10.1002/hyp.6715.

Hall, D. K., A. T. C. Chang, and H. Siddalingaiah (1988), Reflectances of glaciers as calculated using Landsat-5 thematic mapper data, *Remote Sens. Environ.*, *25*(3), 311–312.

Hegde, P., P. Pant, M. Naja, U. C. Dumka, and R. Sagar (2007), South Asian dust episode in June 2006: Aerosol observations in the central Himalayas, *Geophys. Res. Lett.*, *34*, L23802, doi:10.1029/2007GL030692.

Kokhanovsky, A. A., and F. M. Breon (2012), Validation of an Analytical Snow BRDF Model Using PARASOL Multi-Angular and Multispectral Observations, *IEEE Geosci. Remote Sens. Lett.*, *9*(5), 928–932, doi:10.1109/LGRS.2012.2185775.

Lau, K. M., M. K. Kim, and K. M. Kim (2006), Asian monsoon anomalies induced by aerosol direct forcing: The role of the Tibetan Plateau, *Clim. Dyn.*, *26*, 855–864, doi:10.1007/s00382-006-0114-z.

Lau, K. M., M. K. Kim, K. M. Kim, and W. S. Lee (2010), Enhanced surface warming and accelerated snowmelt in the Himalayas and Tibetan Plateau induced by absorbing aerosols, *Env. Res. Lett.*, *5*, 025204, doi:10.1088/1748-9326/5/2/025204.

Levy, R. C., L. A. Remer, R. G. Kleidman, S. Mattoo, C. Ichoku, R. Kahn, and T. F. Eck (2010), Global evaluation of the Collection 5 MODIS dark-target aerosol products over land, *Atmos. Chem. Phys.*, *10*, doi:10.5194/acp-10-10399-2010.

Meehl, G. A., J. M. Arblaster, and W. D. Collins (2008), Effects of black carbon aerosols on the Indian monsoon, *J. Clim.*, *21*, 2869–2882, doi:10.1175/2007JCLI1777.1.

Painter, T. H., J. S. Deems, J. Belnap, A. F. Hamlet, C. C. Landry, and B. Udall (2010), Response of Colorado River runoff to dust radiative forcing in snow, *Proc. Natl. Acad. Sci. U. S. A.*, *107*, 17,125–17,130, doi:10.1073/pnas.0913139107.

Painter, T. H., A. C. Bryant, and S. M. Skiles (2012), Radiative forcing by light absorbing impurities in snow from MODIS surface reflectance data, *Geophys. Res. Lett.*, in press, doi:10.1029/2012GL052457.

Prasad, A. K., and R. P. Singh (2007), Changes in Himalayan snow and glacier cover between 1972 and 2000, *Eos Trans. AGU*, *88*(33), 326, doi:10.1029/2007EO330002.

Qian, Y., M. G. Flanner, L. R. Leung, and W. Wang (2011), Sensitivity studies on the impacts of Tibetan Plateau snowpack pollution on the Asian hydrological cycle and monsoon climate, *Atmos. Chem. Phys.*, *11*, 1929–48, doi:10.5194/acp-11-1929-2011.

Ramanathan, V., C. Chung, D. Kim, T. Bettge, L. Buja, J. T. Kiehl, W. M. Washington, Q. Fu, D. R. Sikka, and M. Wild (2005), Atmospheric brown clouds: Impacts on South Asian climate and hydrological cycle, *Proc. Natl. Acad. Sci. U. S. A.*, *102*, 5326–5333, doi:10.1073/pnas.0500656102.

Ramanathan, V., M. V. Ramana, G. Roberts, D. Kim, C. E. Corrigan, C. E. Chung, and D. Winker (2007), Warming trends in Asia amplified by brown cloud solar absorption, *Nature*, *448*, 575–578, doi:10.1038/nature06019.

Rittger, K., T. H. Painter, and J. Dozier (2012), Assessment of methods for mapping snow cover from MODIS, *Adv. Water. Res.*, in press, doi:10.1016/j.advwatres.2012.03.002.

Salomonson V. V., and I. Appel (2004), Estimating the fractional snow covering using the normalized difference snow index, *Remote Sens. Environ.*, *89*, 351–360, doi:10.1016/j.rse.2003.10.016.

Thompson, L. G., T. Yao, E. Mosley-Thompson, M. E. Davis, K. A. Henderson, and P.-N. Lin (2000), A high-resolution millennial record of the South Asian monsoon from Himalayan ice cores, *Science*, *289*, 1916–1919.

Vermote, E. F., D. Tanré, J. L. Deuzé, M. Herman, and J. J. Mocrette (1997), Second simulation of the satellite signal in the solar spectrum, 6S: An overview, *IEEE Trans. Geosci. Remote Sens.*, *35*(3), 675–686.

Vermote, E. F., N. Z. El Saleous, and C. O. Justice (2002), Atmospheric correction of MODIS data in the visible to middle infrared: First results, *Remote Sens. Environ.*, *83*, 97–111.

Wang, C., D. Kim, A. M. L. Ekman, M. C. Barth, and P. J. Rasch (2009), Impact of anthropogenic aerosols on Indian summer monsoon, *Geophys. Res. Lett.*, *36*, L21704, doi:10.1029/2009GL040114.

Warren, S. G., and R. E. Brandt (2008), Optical constants of ice from the ultraviolet to the microwave: A revised compilation, *J. Geophys. Res.*, *113*, D14220, doi:10.1029/2007JD009744.

Warren, S. G., and W. J. Wiscombe (1980), A model for the spectral albedo of snow. II: Snow containing atmospheric aerosols, *J. Atmos. Sci.*, *37*, 2734–2745.

Wiscombe, W. J., and S. G. Warren (1980), A model for the spectral albedo of snow. I: Pure snow, *J. Atmos. Sci.*, *37*, 2712–3.

Xu, B., et al. (2009), Black soot and the survival of Tibetan glaciers, *Proc. Natl. Acad. Sci. U. S. A.*, *106*(52), 22,114–22,118, doi:10.1073/pnas.0910444106.

Yasunari, T. J., R. D. Koster, K.-M. Lau, T. Aoki, Y. C. Sud, T. Yamazaki, H. Motoyoshi, and Y. Kodama (2011), Influence of dust and black carbon on the snow albedo in the NASA Goddard Earth Observing System version 5 land surface model, *J. Geophys. Res.*, *116*, D02210, doi:10.1029/2010JD014861.

Yasunari, T. J., Q. Tan, K.-M. Lau, P. Bonasoni, A. Marinoni, P. Laj, M. Ménégoz, T. Takemura, and M. Chin (2012), Estimated range of black carbon dry deposition and the related snow albedo reduction over Himalayan glaciers during dry pre-monsoon periods, *Atmos. Environ.*, in press, doi: 10.1016/j.atmosenv.2012.03.031.